Proposal to Jefferson Lab PAC 43

The sidereal time variations of the Lorentz force and maximum attainable speed of electrons

B. Wojtsekhowski (spokesperson-contact), A. Hutton, A. Freyberger, C. Keppel, and Y. Roblin (co-spokesperson)
Thomas Jefferson National Accelerator Facility, Newport News, VA 23606

B. Vlahovic
North Carolina Central University, Durham, NC 27707

K. Allada and B. Schmookler
Massachusetts Institute of Technology, Cambridge, MA 02139

G. Franklin and B. Quinn
Carnegie Mellon University, Pittsburgh, PA 15213

May 17, 2015

Contents

Abstract

We propose an experiment to measure directional variation of the Lorentz force, LF, by means of high precision monitoring of the beam orbit in a high energy particle accelerator. Such a type of experiment has not been performed before. The projected limit on directional variation of the LF from the proposed experiment will be by several orders better than could be estimated from available accelerator records. The results of the experiment, when interpreted in the kinematical framework, will provide a constraint on the anisotropy of the maximum attainable speed (MAS) of electrons. Within a few months of mostly parasitic data taking, the accuracy on the MAS anisotropy should be on the level of 10^{-16}, or 100 times better compared with the current best limit of 10^{-14}. The potential reach could be even more dramatic depending on the stability of the magnets and beam position monitor characteristics, which would be studied in the proposed experiment.

The JLab accelerator beam, due to its parameters (energy, intensity, and emittance), provides a unique tool for the investigation of the MAS via the momentum ratio measurement within the magnetic arc.

In the proposed experiment we will use a kinematical framework for the result analysis and perform a precision test of a postulate of the Special Relativity theory by searching for a sidereal variation of the ratio of the momenta of the electrons moving in different (close to opposite) directions in the magnetic arc(s). This pilot measurement will require only high speed recording of the beam position data with already available equipment and a few dedicated calibrations of the magnetic optics with a total beam time request of 80 hours.

1 Introduction

The invariance of the laws of physics with respect to continuous or discrete transformations presents a keystone of our current concept of nature, and so precision tests of the laws' invariance are recognized as an important way to search for new physics.

A concept of the maximum attainable speed, usually associated with the speed of light, plays a central role in modern physics. The key postulate of Special Relativity, SR, is the isotropy of the maximum attainable speed, MAS, and its constancy in all reference systems. The Lorentz invariance of physics presents one of the fundamental symmetries of nature. It is expected that at the Plank energy scale a violation of SR could happen, and this has motivated a search for precision methods to test the postulate of SR. Development of the unified theory of fundamental forces requires taking into account the quantum theory of a gravitational field, QG. The onset of the QG effects leads to modification of the momentum-energy relationship, which effectively violates the SR postulate on the level defined by the Plank mass, M_P.

A larger number of high precision tests of SR have been performed during the 128 years since the Michelson-Morley experiment in 1887, see review [1]. For evaluation of the SR test experiments, a framework of effective field theory, the Standard Model Extension, was formulated by A. Kostelecky and collaborators [2]. For electro-magnetostatics a minimal SME, mSME, was developed and used to analyze a large body of recent experiments [3]. The current formulation of the mSME allows investigation of the Lorentz invariance violation, LIV, in the photon sector, but the Lorentz force was left as conventional. Such a restriction is very productive in the study of the LIV in the photon sector but unfortunately excludes application of the current mSME to an experiment based on the Lorentz force variation being measured.

There is an earlier proposed test theory where the Lorentz transformations are generalized and the deviation from SR is characterized by a few parameters [4]. This approach, the Robertson-Mansouri-Sexl test theory, RMS, could be directly applied to the proposed experiment. However, the RMS test theory includes only kinematical transformations, which leaves the dynamic aspects of physics including the Lorentz force modification unknown.

A concept of this experiment, discussed in Ref. [5], is based on a measurement of the sidereal time variation of the beam momenta at opposite ends of the 180° magnetic arc. We will use an analysis logic of the proposed experiment based on a combination of the parity conservation in electromagnetic interaction and the kinematical framework RMS.

The status of the experimental investigation of the directional anisotropy of the maximum attainable speed and other LI violations is reviewed regularly, see e.g. [6]. The highest sensitivity to LIV, achieved in an experiment with a rotating pair of microwave cavities [7], is of 10^{-18} for even-parity sidereal variation or the two-way speed of light. The study of odd-parity variation requires a different experimental approach. The strict limit for this type of LIV, obtained by a novel method of Compton backscattering from high energy electrons [8], is of 10^{-14}. A similar level was recently obtained via an asymmetric optical ring [9].

2 Physics concept

The experiment under discussion studies the trajectory of a moving charge in a static magnetic field. The direction of the movement is normal to the direction of the field. The particle trajectory is deflected by a 180° magnetic arc. The experiment measures the radii of the trajectory at the beginning and at the end of the arc. The coordinate system is selected so that the momentum is directed to a positive z at the beginning of the arc and to a negative z at the end of the arc.

Two beam momentum monitors at opposite sides of a 180° bending magnet allow one to measure the ratio of the particle momenta p_+, p_- moving in opposite directions, $R = p_+/p_-$ (see Fig. 1).

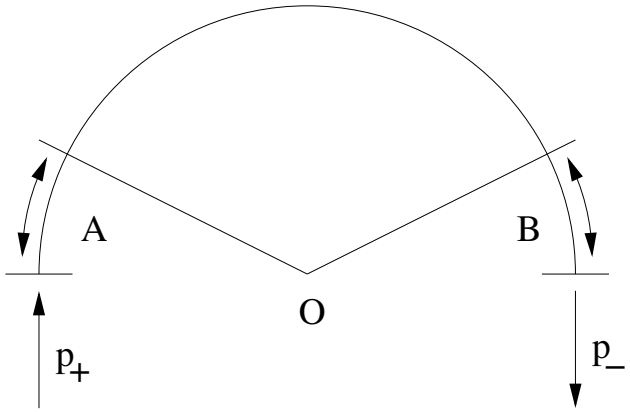

Figure 1: Diagram for measurement of the beam momenta with a 180° arc magnet.

Assuming that there are no acceleration elements between these two momentum measurements and a small correction (calculable) on the radiative energy loss, such a ratio should be stable even when the actual beam energy varies. Moreover, the energy loss due to synchrotron radiation will not be correlated to the sidereal time and hence, not affect the end result. Over time, the average energy loss will converge to the expected value and contribute to the width of the distribution for the the value of R. This value will be very close to 1. The width of that distribution will be mainly due to mis-powerings of the dipole power supplies and systematic errors on the BPM resolution.

The configuration could use a large portion of the arc used as a momentum monitor (the area A (B) shown in Fig. 1) because it allows higher dispersion and better sensitivity in spite of the angle's being smaller than 180° between the two momentum monitors.

In the proposed scheme of experiment the use of the conventional Lorentz force, LF, for the entire magnetic arc leads to a constant value of velocity and a constant value of the total momentum all along the arc because the conventional Lorentz force is orthogonal to both the vector of speed and the vector of momentum. If the maximum attainable speed, MAS, is different for the particle moving in the directions +z and -z, a constant value of the particle velocity means a change in the momentum, but a constant value of the momentum means a change in the velocity. This contradiction means that the modification of the MAS requires some modification of the LF.

We can also see the same from the field theory perspective: The LF describes the interaction of the electrical charge with the electromagnetic field. In the framework of Special Relativity, the LF could be derived with four-vector formalism from the action as follows [10]:

$$S = \int_a^b (-mcds - \frac{e}{c} A_\mu dx^\mu). \tag{1}$$

The Lagrangian is $L = -mc^2\sqrt{1-\beta^2} + \frac{e}{c}\vec{A}\vec{v} - e\phi$ and the generalized momentum is $\vec{P} = \frac{m\vec{v}}{\sqrt{1-\beta^2}} + \frac{e}{c}\vec{A}$. Using the Euler-Lagrange equation

$$\frac{d}{dt}\frac{\partial L}{\partial \vec{v}} = \frac{\partial L}{\partial \vec{r}}, \tag{2}$$

it is easy to get the equation of motion:

$$\frac{d\vec{p}}{dt} = -\frac{e}{c}\frac{\partial \vec{A}}{\partial t} - e\nabla\phi + \frac{e}{c}[\vec{v} \times rot\vec{A}], \tag{3}$$

which contains the usual LF force e.g. for magnetostatics as: $\frac{d\vec{p}}{dt} = \frac{e}{c}[\vec{v} \times rot\vec{A}]$. Such an explicit connection explains our interest in the proposed precision LF measurement. If any variation in LF is observed, a modification of the Lorentz transformation is required. Complementarily, a variation of the maximum attainable speed would likely lead to modification in the LF.

2.1 Maximum attainable speed

For a particle with the speed v, the kinematics can be fully characterized by the value of the maximum attainable speed, MAS, which is usually assumed to be equal to the speed of light c. We will keep the same notation but refer to the MAS of an electron when it is essential. The MAS value defines a Lorentz factor, γ, as:

$$\gamma = \frac{1}{\sqrt{(1-(v/c)^2)}} = \frac{c}{\sqrt{(c-v)\cdot(c+v)}} \tag{4}$$

A very small variation in the difference $v - c$ could be observed via a modestly accurate measurement of the γ factor due to the amplification factor γ^2, as it is easy to see from:

$$\frac{\delta(c-v)}{c} = -\frac{1}{\gamma^2} \times \frac{\delta\gamma}{\gamma} \tag{5}$$

Below we present a possible experiment in which the value of particle speed v is kept constant and allows a search for a possible variation of c with very high precision.

2.2 Experiment analysis and interpretation

In spite of the lack of a dynamic theory of magnetostatics with LIV effects, we can analyze the proposed experiment by using the following two assumptions:

- The P-parity is conserved in the electromagnetic interactions.
- The charged particle motion in a constant magnetic field with a fixed value of the maximum attainable speed is described by the conventional Lorentz force.

It is important to note that in the case of LIV effects, a modification of the energy-momentum dispersion equation is expected, and momentum constancy in the arc is not required. At the same time energy conservation should be preserved.

The action between the charged particle and magnetic field leads to a change in the particle motion. The direction of the action could be found from the direction of particle speed $\vec{v}/|\vec{v}|$ and the direction of the magnetic field $\vec{B}/|\vec{B}|$. Due to the parity conservation requirement and pseudo-vector property of the magnetic field, the vector product operator should be used, which means that the direction of action is orthogonal to the direction of the particle speed. This last conclusion leads to a constant velocity of the particle $|\vec{v}|$. The last result allows us to bridge the momentum measurements performed with the particle moving in opposite directions. For each momentum measurement, the trajectory bend radius R is:

$$R = \frac{m\ v}{\sqrt{(1-(v/c)^2)}} \times \frac{c}{eB}, \tag{6}$$

where the value of the MAS, c, is fixed at a given measurement. The experimental observable is a ratio of the radii measured at opposite locations:

$$R_{A:B} = \frac{R_{A}}{R_{B}} = \frac{\sqrt{1-(v/c_{B})^2}}{\sqrt{1-(v/c_{A})^2}} \times \frac{B_{B}}{B_{A}} \tag{7}$$

We will perform the measurement at different sidereal moments $\omega_{\oplus}t$ and analyze the data by using a fit $c = c_{av} \times [1 + \epsilon \times \cos(\omega_{\oplus}t + \phi)]$, where the average MAS $c_{av} = (c_{A} + c_{B})/2$, the sidereal frequency is $\omega_{\oplus}$, the relative variation of MAS is $\epsilon = \delta c/c_{av}$, and the phase shift is ϕ. Because the $\epsilon \ll 1$ the time dependent part of the ratio $R_{A:B}$ (assuming perfect stability of the magnetic field) could be presented as:

$$\tilde{R}_{A:B} = \frac{\sqrt{1-v/c_{B}}}{\sqrt{1-v/c_{A}}} \tag{8}$$

Assuming that $\epsilon \ll (1 - v/c_{av})$, the expression could be simplified even more:

$$\begin{aligned} \tilde{R}^2_{A:B} &= 1 + \frac{c_{av}}{c_{av}-v}\,\epsilon \times [\cos(\omega_{\oplus}t + \phi_{B}) - \cos(\omega_{\oplus}t + \phi_{A})] = \\ &= 1 - \gamma^2_{av} \times 2\epsilon \cdot \sin(\omega_{\oplus}t + \phi_{A}) \end{aligned} \tag{9}$$

Finally, the variation of the $R_{A:B}$ is related to the MAS variation as: $\delta\tilde{R}_{A:B} = -\gamma^2\,\delta c/c_{av}$.

2.3 Accuracy of magnetic deflection measurement

Measurement of the momentum of a charged particle could be accomplished by using the deflection of its trajectory in the magnetic field. High precision could be achieved by the use

of a large number of particles in the beam as the particles in the beam bunch have a small momentum spread (about 10^{-4} for CEBAF in the highest ARC at 12GeV). Determination of the trajectory requires the measurements of the beam position at at least three points along the beam path. There are about 20-30 beam position monitors in each arc of the CEBAF accelerator.

The precision beam position monitor, BPM, is a non-destructive device based on so-called antenna pick up electrodes. It provides four pick up signals and allows determination of both transverse coordinates of the beam at the location of the BPM. The accuracy of coordinate measurement is defined by the ratio of beam induced signal to electronic noise in the selected frequency range and the size of the opening between the pick up electrodes in the selected frequency range. The achievable precision of a single BPM measurement for a beam current of 100 μA is about 1 μm with 1 ms integration time. At lower beam intensity the accuracy will decrease: 10 μm for a beam of 10 μA.

Magnetic optics allows us to relate the beam position to the beam momentum deviation from the nominal value of the momentum. For initial discussion of the beam momentum measurement in the accelerator, we will use the beam motion equation in terms of the dispersion function η:

$$x(s) \; = \; x_\beta(s) \; + \; \eta(s) \times \frac{\Delta p}{p_n}, \tag{10}$$

where s is a coordinate along the trajectory, $x_\beta(s)$ is the deviation of horizontal position due to betatron oscillation, $\eta(s)$ is a dispersion function, and $\Delta p/p_n$ is the relative deviation of the momentum from the nominal value p_n.

The dispersion function in CEBAF arc#10 reaches about 2.5 m in the dipoles, see Fig. 2. By inverting equation 10 we can estimate that the momentum measurement will have a precision on the level of 1×10^{-6} at 100 μA current. This accuracy should be interpreted only for relative variation because the absolute geometry and field integrals in the arcs are not well known. The outline of the actual procedure for the momentum determination with full account for magnetic optics is presented in Section 4.

2.4 From the stability of the bend radius to the limit of the speed of light variation

The signal of interest has a period of almost 24 hours, which means that about 10^8 measurements would be done during one period, bringing statistical precision of the average momentum (and its variation) to the level of a few 10^{-10}. A corresponding level of sensitivity to the maximum attainable speed variation could be evaluated in the kinematical framework (admitting that it is not a dynamic theory). A variation of MAS as small as 10^{-18} could be observed if magnetic system instability noise at a period of 24 hours is 10^{-10}.

The beam energy could change on the level of 10^{-5} several times over one day. However, as we proposed in Ref. [5], the ratio of the beam momenta at two almost opposite points on the arc allows us to cancel out the impact of the beam energy variation in the proposed search of the sidereal time variation of the momentum.

The remaining key problem of the experiment is the instability of the magnetic system

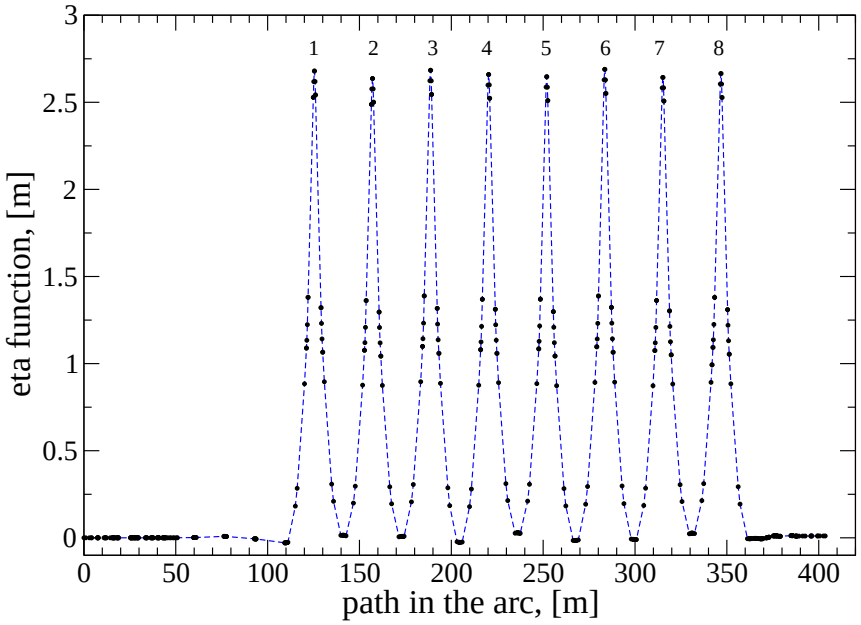

Figure 2: Dispersion function in CEBAF arc#10.

characteristics whose full evaluation requires an empirical study.

A run as long as three months would allow 100 oscillations and bring the desirable stability level down to 10^{-8} over one day. However, considering that the goal of the current proposal for $\delta c/c$ is 10^{-16}, the required stability is on the level of 10^{-6} per day. An even better magnetic system stability of 10^{-7} has been demonstrated in the storage ring electron-positron accelerator VEPP-2m, during a several-week-long electron-positron $g-2$ experiment [12].

3 Experimental Setup

CEBAF (Continuous Electron Beam Accelerator Facility) is a superconducting facility located in Newport News, Virginia, which provides a continuous electron beam of up to 12 GeV for use in nuclear physics experiments in up to four experimental halls simultaneously. The beam is generated at the electron gun equipped with a GaAs photocathode. A circularly polarized laser beam impinges on this cathode and allows polarized electrons to be produced with a longitudinal polarization in excess of 85% and currents as high as 200 μA. Initially at 130 keV of kinetic energy, the electrons are accelerated, bunched and compressed in the injector to an energy of a few tens of MeV depending on the linacs gain and the desired energies in the experimental halls. In its present configuration, CEBAF can thus deliver beams with energy up to 12 GeV.

The acceleration is achieved via two superconducting linacs, set in an anti-parallel configuration and connected by asynchronous recirculation arcs. The delivery of beams of very high quality, with an energy spread of less than a few 10^{-4}, and geometric emittance on the order of a few 10^{-9} mrad, was routinely achieved in the 6 GeV machine and is under commissioning in the 12 GeV configuration.

3.1 The magnetic system

We propose to carry out measurements in the recirculation arcs where the beam energy is constant (to the degree of a stable and calculable synchrotron radiation energy loss). These arcs are isochronous and achromatic. They are designed to bend the beam 180 degrees and present it to the subsequent linac. There are five arcs on each side (east and west) of the machine to recirculate the beam at every pass. Each arc carries a single beam. This is achieved via a spreader which directs the beam to the proper arc for a given pass, as well as a symmetric re-combiner which re-injects it into the next linac.

The first two arcs are made up of 16 dipoles and quadrupoles arranged in a singlet/triplet pattern to form four super-periods. These arcs have high dispersion (up to 8 m in arc#2), and are instrumented with synchrotron radiation monitors for assessment of the longitudinal beam optics. They are also used as the energy reference against which we adjust the linacs. The other arcs feature 32 dipoles and an equivalent set of quadrupoles arranged in the same singlet/triplet pattern. Dipoles define the layout while quadrupoles define the beam envelope and allow for tuning the dispersion, momentum compaction and phase advances.

Power supply Dipoles in the given arc are powered in series by a single power supply (arc bus). During the 12 GeV upgrade, these dipoles were retrofitted with extra return steel to elevate the field saturation that would occur when running at higher excitation. Consequently, the field map for each one was carefully remeasured in the magnet test stand. Dipoles were then paired to minimize orbit distortions in between dipole pairs.

Small corrector dipoles which can be individually adjusted are installed in the arcs to compensate for these remaining orbit variations. They are available for both the horizontal and vertical planes.

The control system utilizes a single field map for all of the dipoles in a given arc forming

the relationship between the power supply current and the integrated magnet field along its nominal trajectory.

Field hysteresis Both dipole and quadrupole magnets exhibit hysteresis. This is not an impediment to reproducibility since we have standard cycling procedures allowing for placing the magnets on the same portion of the hysteresis curve any time they are set.

Field monitoring For all the magnets, the current read backs from their power supplies are monitored and archived as EPICS variables. Depending on the power supply under consideration there is a granularity inherent in the digitization of the analog signals by the ADC. This so-called "bit noise" is on the order of a few mA on the arc power supplies. The set point is on the order of a few hundreds of amps. The relative stability, however, is much better, on the order of a few 10^{-6}.

3.2 The beam position monitors

The CEBAF beam position monitors (BPM) are based on a thin-wire pickup consisting of four 1/4 wave antennas placed parallel to the beam [13]. They are sensitive over a wide range of current (from 1 to 100 μA or more) and linear over 8 mm or so from their electrical center, which is the nominal beam position location in most instances. A heterodyne front-end preamplifier is located in the tunnel near the BPM vessel. After amplification, the pickup signals are down converted and sent upstairs to the service building. A synchronous amplitude detector provides the conversion to amplitude for each antenna. Over the years, subsequent versions of the electronics have significantly improved the sensitivity of the system by reducing the electronic noise and taking maximum advantage of the dynamic range. Parameters such as beam current, integration time and beam pulse structure all affect the outcome. For typical operating conditions, we expect approximately 100 μm of accuracy single-shot. In the arc itself, the 4-channel BPM system averages about 16 measurements, yielding close to a 25 μm accuracy. The result is transmitted to the EPICS control system and updated every second.

By averaging over time, the short term fluctuations of the orbit are washed out and one can determine the beam position with micrometer accuracy. Parity experiments have successfully made use of this in the past [14].

3.3 The data recording system

We use a private version of the MYA archiver [15] to archive all the parameters relevant to the experiment. These include the BPM positions, magnet set points and read back (dipoles, quadrupoles, and correctors) as well as other useful information (beam current, beam mode, etc.). With few exceptions, the vast majority of these channels are already routinely recorded by the production archiver. Unlike the standard archiver, there is no archiving threshold on any of the channels.

4 Data Analysis

As previously described in Section 2.2, we have to determine the momentum of the beam at the start and the end of the arc. The beam line is instrumented with a number of BPMs allowing us to determine the deviations of the orbits from the reference momentum P_0, which is set by the magnetic field in the arc dipoles ($P_0 = B\,\rho$, in proper units).

The deviation from the reference momentum δP can be extracted from knowledge of the beam positions and the transport optics in that region. Denoting by x_a, $x_a^{'}$ and δ, the position, angle and momentum deviation at the entrance of the arc, we can express the orbit at any subsequent BPM by the equations of transport. These depend on the layout of the beam line and the powering of the magnet, both of which are known.

At first order in transport, one can express the deviation at any BPM relative to another location in terms of the expansion:

$$x_i =< X|X > X_a + < X|X^{'} > X_a^{'} + < X|\delta > \delta \tag{11}$$

In the rest of the discussion, we will use the standard matrix notation describing the coefficients of transport and rewrite equation 11 as $x_i = M_{11}X_a + M_{12}X_a^{'} + M_{16}\delta$.

Determining the incoming beam parameters can be achieved via a least-square minimization with the following χ^2:

$$\chi^2 \;=\; \sum_i \Big(X_i - M_{11}X_a - M_{12}X_a^{'} - M_{16}\delta\Big)^2 \tag{12}$$

The least-square minimization will find $\begin{pmatrix} X_a \\ X_a^{'} \\ \delta_a \end{pmatrix}$ at the anchor point such that

$$\tfrac{\partial\chi^2}{\partial X_a} = \tfrac{\partial\chi^2}{\partial X_a^{'}} = \tfrac{\partial\chi^2}{\partial\delta_a} \;= 0.$$

Evaluating the partial derivatives yields:

$$\begin{array}{lllllllllll}
\sum\limits_i \left(M_{11}^{ai\,2}\right) & X_a & + & \sum\limits_i (M_{11}^{ai}M_{12}^{ai}) & X_a^{'} & + & \sum\limits_i (M_{11}^{ai}M_{16}^{ai}) & \delta_a & = & \sum\limits_i (M_{11}^{ai}X_i) \\
\sum\limits_i (M_{11}^{ai}M_{12}^{ai}) & X_a & + & \sum\limits_i \left(M_{12}^{ai\,2}\right) & X_a^{'} & + & \sum\limits_i (M_{12}^{ai}M_{16}^{ai}) & \delta_a & = & \sum\limits_i (M_{12}^{ai}X_i) \\
\sum\limits_i (M_{11}^{ai}M_{16}^{ai}) & X_a & + & \sum\limits_i (M_{12}^{ai}M_{16}^{ai}) & X_a^{'} & + & \sum\limits_i \left(M_{16}^{ai\,2}\right) & \delta_a & = & \sum\limits_i (M_{16}^{ai}X_i)
\end{array}$$

which depends only on the reading on the BPMs (X_i) and the transport coefficients between the start of fit a and each BPM$_i$.

We perform the least square fit of the BPM data for sections of the beam line spanning the first and last dipole. Each region consists of 12 BPMs and encompasses a straight region followed by a bending dipole. The former allows us to gauge the incoming angle and position fluctuations, the latter the deviation from the central momentum set by the dipole.

In order to carry out this analysis one has to read back the powering of the quadrupoles and dipoles in this region. We calculate the beam transport parameters relating the anchor

point of the fit and every subsequent BPM. If we consider only first order motion, we need the M_{11}, M_{12}, M_{16} in the equations above.

Next, the corrector contributions are removed from each BPM. That is, for each corrector in this beam line we calculate the resulting angle and propagate it to subsequent BPMs, yielding the correction:

$\Delta X_b = \sum_c \left(X'_c M_{12}^{cb}\right)$ at each BPM, where c runs over the correctors and b over the BPMs.

Finally, the least square sums are formed and the system inverted for the incoming parameters. The absolute momentum as seen by the dipole can thus be written as $P = P_0(1+\delta_a)$, where the dipole central momentum P_0 is directly related to the bending angle (fixed by the layout) and the powering by $P_0\theta = BL$, where we used $\rho\theta = L$ to express it in terms of the control system parameter BL, which gives the integrated field in the dipole along the trajectory and is directly related to the power supply current via a field map.

This fitting procedure is repeated for the region at the end of the arc, which encompasses the last dipole and is anchored at the second step of the re-combiner. The last step is to calculate $R_{_A}$ and $R_{_B}$ as in equation 9 and fit the data with the sidereal time variation parameter ϵ.

4.1 Validation of the analysis method

We used ELEGANT [16] to simulate the measurement and evaluate the sensitivity of the method. Since the BPMs only sample specific locations of the orbit, even a perfect instrument will result in a residue for the momentum determination. Simulations demonstrate that we are sensitive to a few 10^{-6} in momentum deviation from the nominal. The reconstruction also correctly separates incoming orbit fluctuations from energy errors. Figure 3 shows the error in the reconstruction of the momentum deviation for a thousand randomly generated incoming orbit fluctuations in the first pass of the east arc. It is expressed as the difference between the expected value and the reconstructed value for δ. Note that this represents the best possible case in which BPMs are perfect and the magnets are powered as designed.

Repeating the calculation for the last dipole in the beam line and fitting backwards, anchoring the fit at the R04 BPM, one can calculate the ratio of the momenta R at the opposite sides of the arc.

We also included random incoming orbit variations on the order of 0.5 mm RMS (typical residue during steady running after the slow orbit locks stabilize the orbit). The dominant contribution to the error in this determination of R comes from the stability of the dipole power supply. We assigned a standard deviation of 10 ppm for this contribution in our simulation. This is a reasonable estimate since there are data to support 10 ppm over 24 hours for most of these dipole power supplies. Quadrupole mis-powering is not as critical as it might seem. This is due to the fact that once the alignment between the quadrupole and its associated BPM on the same girder is achieved, the beam mainly samples the center of the quadrupole and therefore does not deflect significantly. We assigned a stability of 10^{-3} to this parameter.

Figure 4 shows the simulated R ratio in arc#1 under the aforementioned conditions for 2 hours of real beam time (one BPM update per second). A total of 10,000 measurements

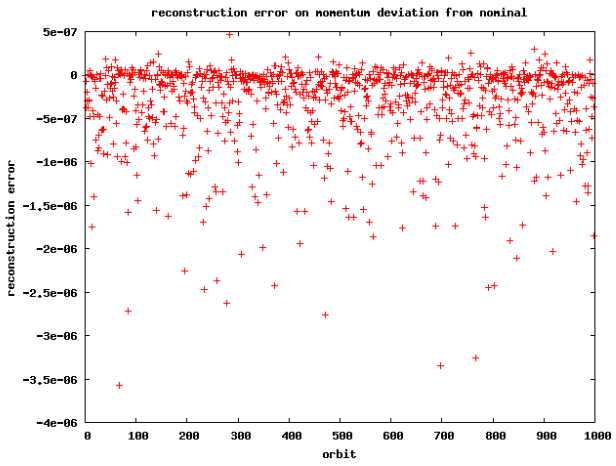

Figure 3: Reconstruction errors in the momentum deviation in the first pass of the east arc.

were analyzed for the presented plot in Fig. 4. The observed RMS of the reconstructed R is $1.1 \cdot 10^{-5}$ which leads to stability of the centroid of the distribution at the level $1.1 \cdot 10^{-7}$ after three-hour measurement.

It can be inferred that the determination of the mean value R is at least on the level of 10^{-6}. This is in line with the goal of the current proposal.

Such a determination should allow us to reach a sensitivity to the MAS variation of about 10^{-15} in 3 hours.

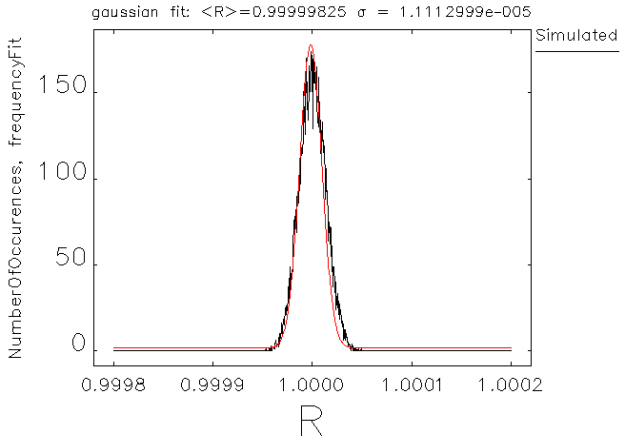

Figure 4: The momenta ratio R in arc#1 in the presence of the magnet mis-powering and incoming orbit fluctuations.

Effect of quadrupole misalignments Quadrupoles are placed on girders and aligned by the survey group on the design layout trajectory with a tolerance of 200 μm in a transverse position. This misalignment does not affect the accuracy with which we can determine the sidereal variations of the R value. Instead, it is a systematic error which shifts the centroid

value of R. We estimated this effect by running simulations with randomly misaligned machines. In order to further reduce this systematic error, it is possible to carefully determine the offset of the quadrupoles in the fitted regions by a beam based measurement [18]. This method can resolve a 200 μm offset with a 5% accuracy. Based on this, we assigned a standard deviation of 50 μm to the misaligment errors in the simulations.

4.2 Optics calibration and monitoring

In order to have confidence in the measurement, we will take special runs at regular intervals for which we vary the energy in the North Linac by driving one or more cavities at a given frequency over a known amplitude. This can be implemented using a technique similar to what is being used for the fast feedback energy modulation system. The advantage of such a method is that one can perform Fourier analysis to pick up that same frequency in the BPMs and therefore get a measurement that is relatively insensitive to sources of fluctuations that are uncorrelated with the energy change. Another alternative readily available for testing is to simply vary the gradient of a cavity via the EPICS control system.

5 Proposed Measurements

5.1 Results of existing data analysis

The beam position data for the CEBAF beam have been recorded since the beginning of operation in 1995. These data could be used for data mining. However, in order to cope with the volume of data, most archived channels are gated by a threshold under which the recording does not occur. The EPICS system itself will report a position change in the BPM each time the signal changes, no matter how small it is. The recording however, is enabled only if the deviation from the previously recorded value is greater than this threshold. It is currently set to 50 μm in the production archiver.

In the fall of 2014, for experimental purposes, the data were recorded in arc#1 without any filter. These data we used to evaluate position resolution and perfect the beam momentum reconstruction algorithm.

5.2 New data collection plan

We propose to carry out this analysis in every arc. However, since the sensitivity to the sidereal variations of the speed of light is proportional to γ^2 (see formula 5 in section 2.1), it is more advantageous to use the high energy arcs. A careful analysis will combine the sidereal time dependent correlations as well as a careful comparison between arcs of different energies since the LIV signal, if such exists, will increase gradually with the beam energy.

Case study for arc#10 The arc#6 through arc#10 are subject to increasing levels of synchrotron radiation. For this reason we have slightly different optics (double bend achromat) to reduce the emittance growth. Ideally, one should also adjust the quadrupoles and dipoles so such that their reference momentum matches that of the beam. As we mentioned before, the CEBAF arcs dipoles are powered in series with no means of individual adjustment. This leads to a significant orbit excursion if not compensated for. In order to control the change of orbit due to the energy loss, coil packages were installed at specific locations to supplement the dipoles [17].

Figure 5 shows the horizontal orbit (in black) with no corrections. The main dipole power supply has been set to the reference momentum corresponding to the middle of the arc. The orbit in red is the result of actuating the correctors to mitigate the excursion. One can see that the correction is imperfect and also takes up most of the corrector capacity (Fig. 7 shows the resulting corrector powering). Activating the coils results in the situation in Fig. 6. Most of the excursion is gone and only minor corrector strengths are required to get a near perfect cancellation.

During production running, we will be in the situation shown in that figure. The current in the coils will be adjusted to cancel most of the orbit deflection and the power supply will be set to the momentum at the center of the arc. For arc#10, this means that the first and last dipoles, where one measures for the ratio R, will be off momentum by about 810^{-4} (The total momentum deviation due to the synchrotron energy loss is approximately 1.610^{-3} over the full arc).

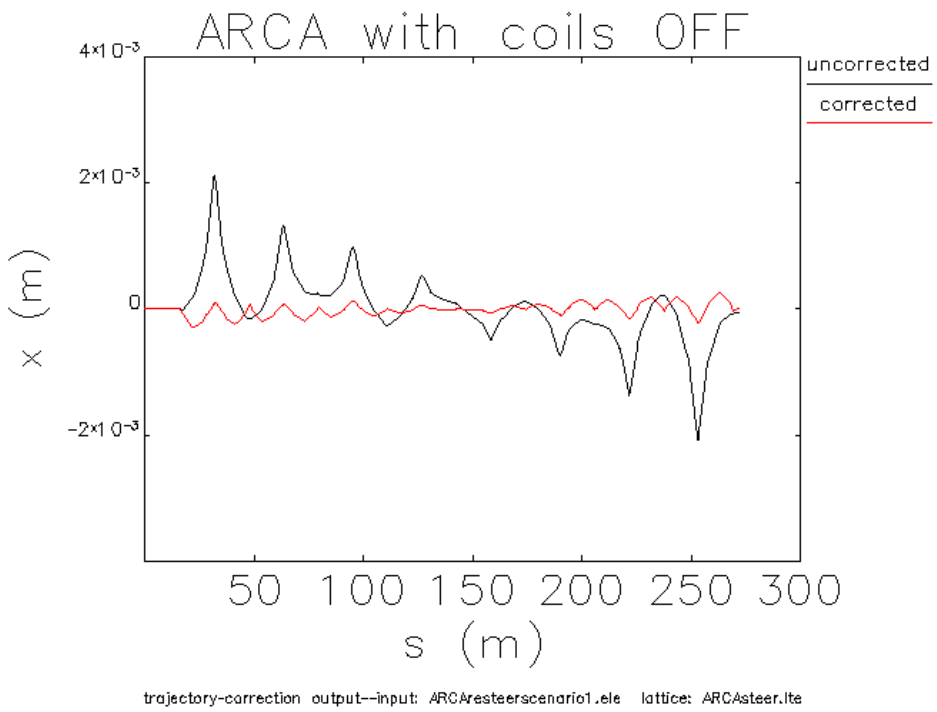

Figure 5: Effect of synchrotron radiation on the orbit in arc#10. The black line represents the expected orbit with no corrections; the red line is the orbit after using the correctors to mitigate the problem.

This does not affect the method we described in section 4. As a matter of fact, this is a more favorable situation since the energy dependent part of the deflection at the dispersive BPM will be greater and hence, less sensitive to orbit related noise.

5.3 Dedicated data collection for calibration

We ask for dedicated beam time in order to verify and calibrate the analysis method.

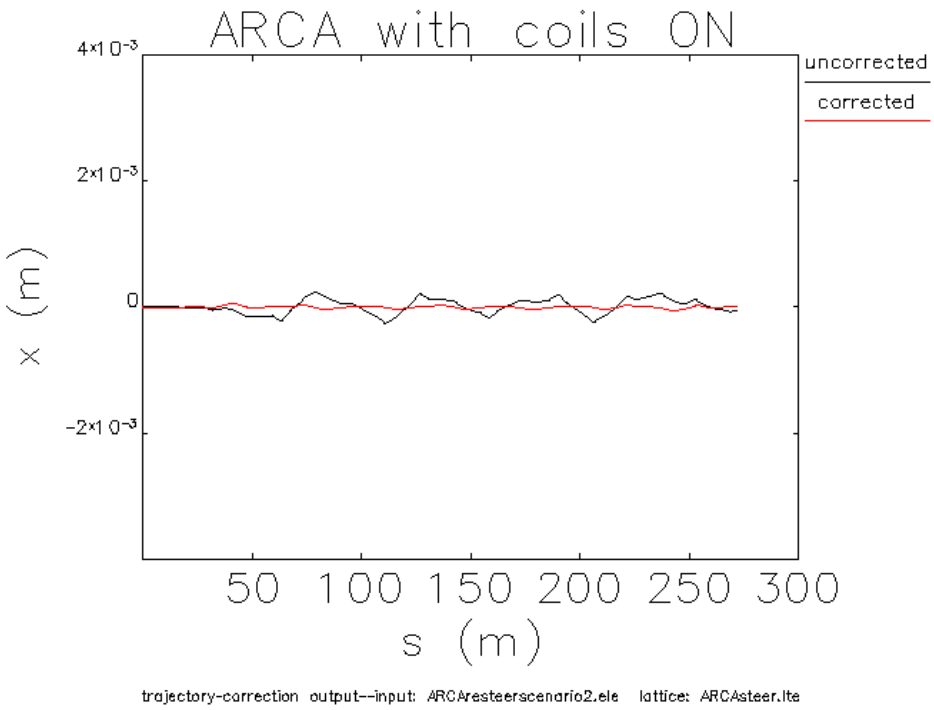

Figure 6: Effect of synchrotron radiation on the orbit in arc#10. The synchrotron radiation compensation coils are on. The black line is the resulting orbit, the red line is the orbit after using the correctors to further mitigate the problem.

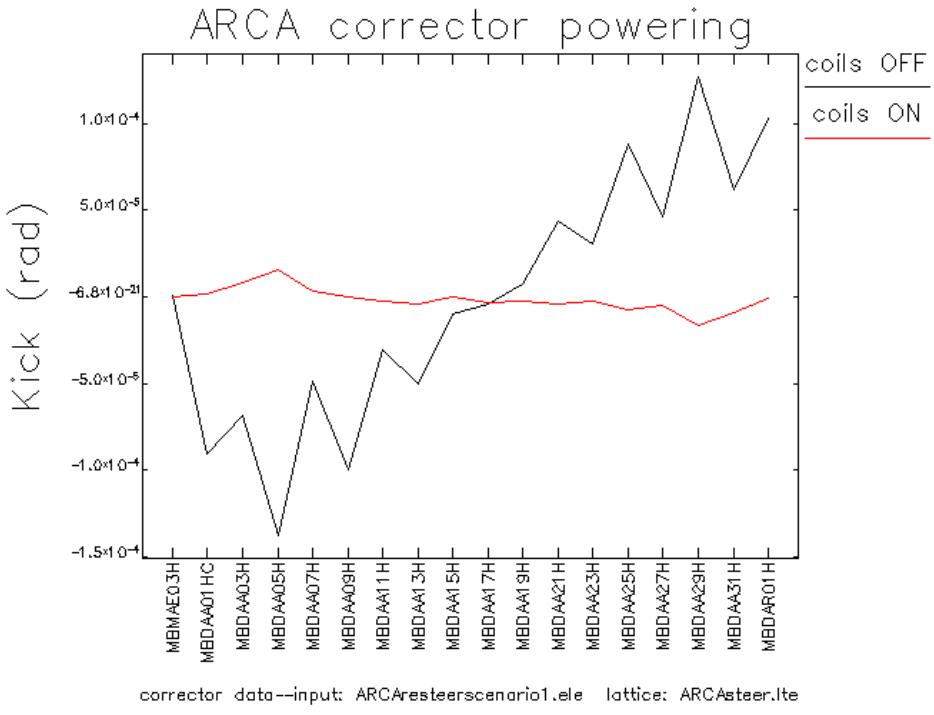

Figure 7: Corrector powering in arc#10 with and without synchrotron radiation coils on.

6 Conclusion

We have proposed a novel experiment to search for sidereal time variation of the Lorentz force by using high energy electron beam deflection in the CEBAF magnetic arc.

We request support from the PAC and approval of 80 hours of beam-time, which will be used for calibration of the magnetic optics and response functions.

The data could be interpreted in terms of sidereal time variation of the maximum attainable speed of the electron and allow at least a 100-times improvement over the current limit on such variation. The potential sensitivity of the proposed method approaches the onset of quantum gravity effects.

References

[1] S. Liberati, Class. Quantum Grav. 30, 133001 (2013).

[2] D. Colladay and V.A. Kostelecký, Phys. Rev. D 55, 6760 (1997);
D. Colladay and V.A. Kostelecký, Phys. Rev. D 58, 116002 (1998).

[3] V.A. Kostelecký and M. Mewes, Phys. Rev. D 66, 056005 (2002);
Q.G. Bailey and V.A. Kostelecký, Phys. Rev. D 70, 076006 (2004).

[4] H.P. Robertson, Reviews of Modern Physics **21 (3)**, 378 (1949); R. Mansouri and R.U. Sexl, Gen. Relativ. Gravit. **8**, 497 (1977); **8**, 515 (1977); **8**, 809 (1977).

[5] B. Wojtsekhowski, European Physics Letters, 108 (2014) 31001.

[6] C.M. Will, The Confrontation between General Relativity and Experiment, arXiv:1403.7377v1.

[7] M. Nagel, S.R. Parker, E.V. Kovalchuk, P.L. Stanwix, J.G. Hartnett, E.N. Ivanov, A. Peters, M.E. Tobar, Direct Terrestrial Measurement of the Spatial Isotropy of the Speed of Light to 10^{-18}, arXiv:1412.6954 [hep-ph].

[8] J.-P. Bocquet *et al.*, Phys. Rev. Lett. **104**, 241601 (2010).

[9] Y. Michimura *et al.*, Phys. Rev. Lett. **110**, 200401 (2013).

[10] L.D. Landau & E.M. Lifshitz, The Classical Theory of Fields.

[11] S. Walston *et al.*, Nuclear Instruments and Methods A **578** 1 (2007); M. Slater *et al.*, Nuclear Instruments and Methods A **592**, 201 (2008); H. Maesaka *et al.*, **696**, 66 (2012).

[12] I.B. Vasserman *et al.*, Physics Letters B, 198/2, 302 (1987).

[13] W. Barry, Nuclear Instruments and Methods A **301**,407 (1991).

[14] Y. Chao et al, 'ACHIEVING BEAM QUALITY REQUIREMENTS FOR PARITY EXPERIMENTS AT JEFFERSON LAB', proceedings of EPAC 2004, Lucerne, Switzerland.

[15] `https://halldweb1.jlab.org/wiki/index.php/Archiver_for_EPICS`

[16] M. Borland, APS LS-287, September 2000.

[17] M. Tiefenback, 'Correction Mechanisms for Synchrotron Radiation Energy Droop in Beam Transport at CEBAF' http://tnweb.jlab.org/tn/2008/08-041.pdf

[18] T. Satogata 'Quadrupole Centering for CEBAF', JLAB TN-14-027, July 2014.